

**SANDIA NATIONAL LABORATORIES
WASTE ISOLATION PILOT PLANT**

**ANALYSIS PACKAGE FOR DIRECT BRINE RELEASE IN THE
2019 COMPLIANCE RECERTIFICATION APPLICATION
PERFORMANCE ASSESSMENT (CRA-2019 PA)**

REVISION 0

Author:	<u>James Bethune</u>		<u>6/4/2019</u>
	Print	Signature	Date
Technical Reviewer:	<u>Brad Day</u>		<u>6/4/2019</u>
	Print	Signature	Date
QA Reviewer:	<u>Shelly Nielsen</u>		<u>6-4-19</u>
	Print	Signature	Date
Management Reviewer:	<u>Chris Camphouse</u>		<u>6/14/2019</u>
	Print	Signature	Date

ERMS #571370

JUNE 2019

WIPP:4.2.1:PA:QA-L:571155

Information Only

This page intentionally left blank.

TABLE OF CONTENTS

EXECUTIVE SUMMARY	V
1.0 INTRODUCTION.....	7
1.1 Changes Since the CRA-2014	8
1.2 Abandonment of Panel Closures in the South	9
2.0 CONCEPTUAL APPROACH FOR THE CRA-2019.....	11
2.1 Model Geometry	12
2.2 Boundary Conditions	13
2.3 Initial Conditions	13
3.0 DBR METHODOLOGY.....	15
3.1 Modeled Scenarios.....	15
3.2 Code Execution and Run Control	15
4.0 RESULTS	17
4.1 Summary.....	17
4.2 S1-DBR.....	20
4.3 S2-DBR.....	22
4.4 S4-DBR.....	24
4.5 Maximum Releases.....	26
5.0 DRIVERS AND CORRELATIONS	27
5.1 Initial Conditions Summary.....	27
5.2 Sensitivity to Initial Conditions	31
5.3 Borehole Size Summary	35
5.4 Sensitivity to Borehole Size.....	36
6.0 SUMMARY	37
7.0 REFERENCES.....	39

LIST OF TABLES

Table 1 – PCS_NO properties.....	9
Table 2 – Summary of parameters used to compute DBR volumes	12
Table 3 – DBR scenarios	15
Table 4 – DBR volume summary	18
Table 5 – S1-DBR volume summary.....	20
Table 6 – S2-DBR volume summary.....	22
Table 7 – S4-DBR volume summary.....	24
Table 8 – Largest DBR volumes by analysis.....	26
Table 9 – S2-DBR mean initial conditions, lower and middle locations.....	28
Table 10 – S2-DBR mean borehole size.....	35

LIST OF FIGURES

Figure 1 – CRA19 DBR grid with simulated intrusion locations.....	13
Figure 2 – Regions used to transfer initial pressure and saturation from the BRAGFLO Salado grid to the DBR grid	14
Figure 3: DBR run control diagram.....	16
Figure 4 – Release volume frequency, all intrusions.....	19
Figure 5 – Release volume boxplots, all non-zero events	19
Figure 6 – S1-DBR release volume boxplots, all intrusions.....	21
Figure 7 – S2-DBR release volumes, all intrusions.....	23
Figure 8 – S4-DBR releases rolumes, all intrusions.....	25
Figure 9 – S2-DBR brine pressure, all lower and middle intrusions.....	29
Figure 10 – S2-DBR brine saturation, all lower and middle intrusions.....	30
Figure 11 – S2-DBR release volume versus brine pressure, all non-zero lower and middle intrusions.....	32
Figure 12 – S2-DBR release volume versus brine saturation, all non-zero lower and middle intrusions.....	33
Figure 13 – Brine saturation frequency, S2-DBR all lower and middle intrusions.....	34
Figure 14 – S2-DBR borehole size, all intrusions	35
Figure 16 – Brine release versus borehole area, S2-DBR	36

Executive Summary

The Land Withdrawal Act requires that the U.S. Department of Energy (DOE) apply for recertification of the Waste Isolation Pilot Plant (WIPP) every five years following the initial 1999 waste shipment. The 2019 Compliance Recertification Application (CRA-2019) is the fourth WIPP recertification application submitted for approval by the U.S. Environmental Protection Agency. A performance assessment (PA) has been executed by Sandia National Laboratories in support of the DOE submittal of the CRA-2019. Results found in the CRA-2019 PA are compared to those obtained in the 2014 Compliance Recertification Application (CRA-2014) in order to assess repository performance in terms of the current regulatory baseline. This package documents the Direct Brine Release (DBR) analysis component of the CRA-2019 PA. Changes incorporated into the CRA-2019 PA include repository planned changes, parameter updates, and refinements to PA implementation. Changes included in the CRA-2019 PA that potentially affect Direct Brine Release results as compared to the CRA-2014 are:

- The lack of ROMPCS in the south end of the repository between Panels 3, 4, 5, 6, and 9, which allows greater brine and gas flow between the lower intrusion and middle intrusion regions
- Modifications, updates, and additions to the BRAGFLO Salado model that affect the initial conditions of the BRAGFLO DBR model
- Modifications to the effective shear strength of waste in the CUTTINGS_S model that affect borehole size in DBR calculations

Overall, the primary impacts of changes for the CRA-2019 PA in comparison to the CRA-2014 PA baseline are substantially higher average DBR event magnitudes and frequencies, and higher maximum DBR volumes. These changes are driven by higher pressures throughout the BRAGFLO DBR modeling domain, and substantially higher saturations in the middle intrusion locations. The increases are accounted for primarily in the scenarios that simulate the effects of a hydraulic connection between a hypothetical brine reservoir underlying the repository and the lower intrusion region. Average DBR volumes from both the lower and middle intrusion locations increased by a similar magnitude, but because middle intrusion events had previously produced much smaller DBR volumes than lower intrusion events, the increase in the middle intrusion DBR volumes represents a much more substantial relative change.

This page intentionally left blank.

1.0 INTRODUCTION

The Waste Isolation Pilot Plant (WIPP), located in southeastern New Mexico, has been developed by the U.S. Department of Energy (DOE) for the geologic (deep underground) disposal of transuranic (TRU) waste. Containment of TRU waste at the WIPP is regulated by the U.S. Environmental Protection Agency (EPA) according to the regulations set forth in Title 40 of the Code of Federal Regulations (CFR), Part 191. The DOE demonstrates compliance with the containment requirements according to the Certification Criteria in Title 40 CFR Part 194 by means of performance assessment (PA) calculations performed by Sandia National Laboratories (SNL). WIPP PA calculations estimate the probability and consequence of potential radionuclide releases from the repository to the accessible environment for a regulatory period of 10,000 years after facility closure. The models used in PA are maintained and updated with new information as part of an ongoing process. Improved information regarding important WIPP features, events, and processes typically results in refinements and modifications to PA models and the parameters used in them. Planned changes to the repository and/or the components therein also result in updates to WIPP PA models. WIPP PA models are used to support the repository recertification process that occurs at five-year intervals following the receipt of the first waste shipment at the site in 1999.

PA calculations were included in the 1996 Compliance Certification Application (CCA) (U.S. DOE 1996), and in a subsequent Performance Assessment Verification Test (PAVT) (MacKinnon and Freeze 1997a, 1997b and 1997c). Based in part on the CCA and PAVT PA calculations, the EPA certified that the WIPP met the regulatory containment criteria. The facility was approved for disposal of transuranic waste in May 1998 (U.S. EPA 1998). PA calculations were an integral part of the 2004 Compliance Recertification Application (CRA-2004) (U.S. DOE 2004). During their review of the CRA-2004, the EPA requested an additional PA calculation, referred to as the CRA-2004 Performance Assessment Baseline Calculation (PABC) (Leigh et al. 2005), be conducted with modified assumptions and parameter values (Cotsworth 2005). Following review of the CRA-2004 and the CRA-2004 PABC, the EPA recertified the WIPP in March 2006 (U.S. EPA 2006).

PA calculations were completed for the second WIPP recertification and documented in the 2009 Compliance Recertification Application (CRA-2009). The CRA-2009 PA resulted from continued review of the CRA-2004 PABC, including a number of technical changes and corrections, as well as updates to parameters and improvements to the PA computer codes (Clayton et al. 2008). To incorporate additional information which was received after the CRA-2009 PA was completed, but before the submittal of the CRA-2009, the EPA requested an additional PA calculation, referred to as the 2009 Compliance Recertification Application Performance Assessment Baseline Calculation (PABC-2009) (Clayton et al. 2010), be undertaken which included updated information (Cotsworth 2009). Following the completion and submission of the PABC-2009, the WIPP was recertified in 2010 (U.S. EPA 2010).

PA calculations were completed for the third WIPP recertification and documented in the 2014 Compliance Recertification Application (CRA-2014). Following the completion and submission of the CRA-2014, the WIPP was recertified in 2017 (U.S. EPA 2017).

The Land Withdrawal Act (U.S. Congress 1992) requires that the DOE apply for WIPP recertification every five years following the initial 1999 waste shipment. The 2019 Compliance Recertification Application (CRA-2019) is the fourth WIPP recertification application submitted by the DOE for EPA approval. The PA executed by SNL in support of the CRA-2019 is detailed in AP-181 (Zeitler 2019). The CRA-2019 PA includes repository planned changes, parameter updates, and refinements to PA implementation. Results found in the CRA-2019 PA are compared to those obtained in the CRA-2014 PA in order to assess repository performance in terms of the current regulatory baseline. This analysis package documents the Direct Brine Release (DBR) component of the CRA-2019 PA analysis.

1.1 Changes Since the CRA-2014

Several changes are incorporated in the CRA-2019 PA relative to the CRA-2014 PA that potentially impact Direct Brine Release results. The changes are:

1. Inclusion of an approach to accommodate the operational decisions to not emplace panel closures in Panels 3, 4, 5, and 6.
2. Inclusion of an approach to accommodate an additional shaft connecting the repository to the surface, as well as an additional mined region in the repository north end to accommodate drifts that lead to the new shaft.
3. Refinement of the gas generation process model to include brine radiolysis.
4. Refinement to the corrosion rates of steel under humid and inundated conditions.
5. Refinement to the effective shear strength of WIPP waste.
6. Refinement to colloid enhancement parameters associated with actinide mobilization.
7. Refinement to the hydromagnesite to magnesite conversion rate.
8. Removal of two chemical reactions associated with iron sulfidation.
9. Correction to the length of the northernmost panel closure representation in the BRAGFLO grid.
10. Updates to WIPP waste inventory parameters.
11. Updates to radionuclide solubilities and their associated uncertainty.
12. An update to the BH_OPEN:RELP_MOD parameter.
13. Computational code updates to BRAGFLO and PREBRAG.

Of the changes listed above, removal of panel closures of the south most directly impacts the DBR volume calculation methodology. This change will be discussed in the following section. Other changes affect the DBR calculations through their effect on pressure and saturation DBR initial conditions generated by the BRAGFLO Salado model, as discussed in Day (2019), or through their effect on the borehole size generated by the cuttings, cavings, and spillings model, as discussed in Kicker (2019). BRAGFLO Salado and DBR parameter values for the CRA-2019 PA analysis (CRA19) are detailed in Kim and Feng (2019).

1.2 Abandonment of Panel Closures in the South

As outlined in the CRA-2019 analysis plan (Zeitler 2019a), operational considerations have prompted the abandonment of plans to emplace run-of-mine salt panel closures (ROMPCS) in Panels 3, 4, 5, 6, and waste in Panel 9. An approach to modeling the impacts of the operational changes is described in Zeitler et al. (2017). The aspects of the APCS approach that are impactful to the BRAGFLO DBR results are the replacement of the ROMPCS in the southernmost panel closure area with a new material, PCS_NO, in both the BRAGFLO DBR model and the BRAGFLO Salado model that provides the BRAGFLO DBR model its initial conditions (Table 1).

Table 1 – PCS_NO properties

Property	Description	Units	Value
CAP_MOD	Model number, capillary pressure model	(-)	1
COMP_RCK	Bulk compressibility	Pa ⁻¹	0
KPT	Flag for permeability determined threshold	(-)	0
PCT_A	Threshold pressure linear parameter	Pa	0
PCT_EXP	Threshold pressure exponential parameter	(-)	0
PC_MAX	Maximum allowable capillary pressure	Pa	1.0E8
PORE_DIS	Brooks-Corey pore distribution parameter	(-)	0.7
POROSITY	Effective porosity	(-)	0.18
PO_MIN	Minimum brine pressure for capillary model KPC=3	Pa	101325
PRESSURE	Brine far-field pore pressure	Pa	101325
PRMX_LOG	Log of intrinsic permeability, X-direction	Log(m ²)	-11
PRMY_LOG	Log of intrinsic permeability, Y-direction	Log(m ²)	-11
PRMZ_LOG	Log of intrinsic permeability, Z-direction	Log(m ²)	-11
RELP_MOD	Model number, relative permeability model	(-)	11
SAT_RBRN	Residual Brine Saturation	(-)	0
SAT_RGAS	Residual Gas Saturation	(-)	0

This page intentionally left blank.

2.0 CONCEPTUAL APPROACH FOR THE CRA-2019

If the WIPP repository were to be penetrated by a borehole while under conditions of sufficient repository brine pressure and saturation, brine could migrate up through the intruding borehole to reach the land surface. Such an event is defined as a direct brine release (DBR). The BRAGFLO DBR analysis uses the BRAGFLO code to numerically evaluate the volumetric flux of brine that enters the borehole over the duration of the release using the well deliverability equations (Mattax and Dalton, 1990):

$$\text{DBR volume} = \int_0^{t_e} q_b(t) dt = \int_0^{t_e} J_b [p_b(t) - p_{wf}] dt \quad (1)$$

In which:

- t_e duration of the DBR event [s] = 4.5 days;
- $q_b(t)$ volumetric flux [m^3/s] of brine to the intrusion as a function of time, t ;
- J_b well productivity index [$\text{m}^3/(\text{Pa}\cdot\text{s})$]
- $p_b(t)$ volume-averaged brine pressure of the repository near the intrusion [Pa]; and
- p_{wf} flowing bottom-hole pressure (FBHP) [Pa].

Values for the flowing bottom-hole pressure, p_{wf} , were previously tabulated through an iterative calculation assuming equilibrium with atmospheric pressure at the ground surface for a range of repository pressures and saturations, then accessed through a lookup table (Stoelzel, 1996).

The well productivity index, J_b , is a measure of how readily brine can enter the well. In a radial drainage area with uniform saturation, it can be determined from Darcy's law (Chappelear and Williamson 1981):

$$J_b = \frac{2\pi k k_r h}{\mu (\ln[r_e/r_w] + s - 0.5)} \quad (2)$$

In which:

- k intrinsic permeability of the waste [m^2];
- k_r relative permeability of the brine [--];
- h height of the crushed panel [m];
- μ brine viscosity [Pa/s];
- r_e effective radius of the intruded cell [m];
- r_w radius of the well [m]; and
- s skin factor [--].

Relative permeability is computed using the model of Brooks and Corey (1964) given by $k_r = S_e^{3+2/\lambda}$ where λ is the pore distribution parameter, $S_e = (S_b - S_{br})/(1 - S_{br})$ is the effective brine

saturation, S_b is the brine saturation, and S_{br} is the residual brine saturation. The crushed panel height is defined as $h = h_i(1 - \phi_i)/(1 - \phi)$, where h_i is initial panel height (fixed at 3.96 m), ϕ_i is the initial room-scale porosity, and ϕ is the room-scale porosity at the time of intrusion, which is calculated by BRAGFLO (see Helton et al. 1998). The effective drainage radius is defined by $r_e = \sqrt{\Delta x \Delta y / \pi}$, where Δx and Δy are the dimensions of the grid cell containing the well. The wellbore radius is fixed at 0.1556 m, which is based on the assumption of a 12.25 in. drill bit diameter.

The parameter values used to compute the DBR volumes are summarized in Table 2.

Table 2 – Summary of parameters used to compute DBR volumes

Parameter	Name in BRAGFLO	Description	Value
k	PRMX	Intrinsic Permeability	$2.4 \times 10^{-13} \text{ m}^2$ (fixed)
λ	PORE_DIS	Brooks-Corey parameter	2.89
S_{br}	SAT_RBRN	Residual brine saturation	Uniform distribution Max: 0.552 Mean 0.276 Min 0.000
ϕ_i	POROSITY	Initial panel porosity	0.848
μ	VISCO	Brine dynamic viscosity	0.0021 Pa-s

As defined for WIPP PA, minimum pressure and saturation conditions must exist within the waste panel for brine to flow to the surface during an intrusion and produce a DBR. Pressure in the intruded waste panel must be great enough to overcome the static pressure exerted by a column of drilling fluid at the repository depth, assumed to be equal to 8 megapascals (MPa). Brine saturation in the intruded waste panel must be above the residual brine saturation of the waste (a sampled parameter), i.e., the brine must be mobile.

2.1 Model Geometry

The BRAGFLO_DBR model explicitly represents the vicinity of the waste panels, including specific repository features like individual panels and panel closures, in a 2-dimensional rectilinear grid. Like the BRAGFLO Salado Model, the grid dips 1° to the south. The DBR numerical grid and material map used in the CRA-2019 PA calculations are shown in Figure 1. Relative to the CRA-2014 DBR grid, the CRA-2019 grid has replaced eight of the panel closures in the south end of the mine with the material PCS_NO, a material intended to capture the absence of panel closures (Zeitler et al. 2017). The same three drilling locations considered in the CRA-2014 PA are considered in the CRA-2019 PA, namely: upper (up-dip), middle, and lower (down-dip) locations. They are shown in Figure 1.

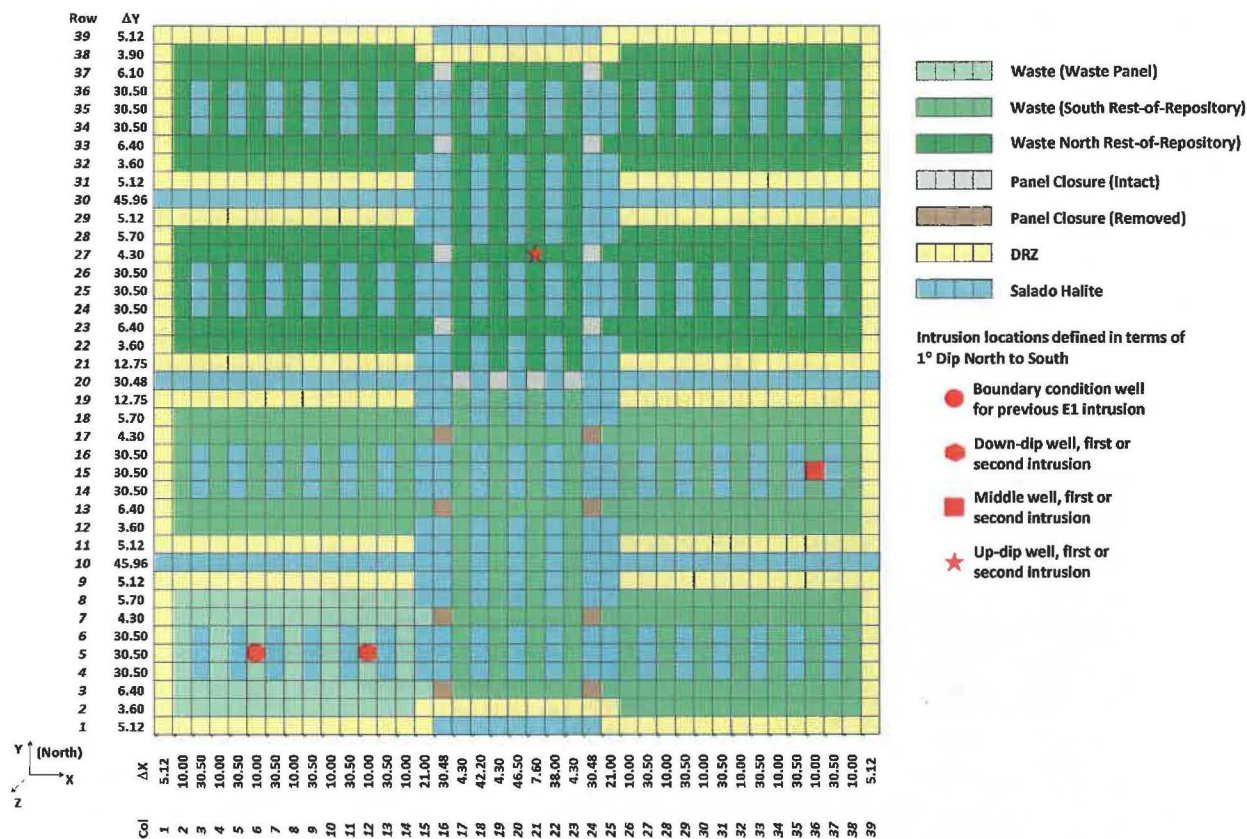


Figure 1 – CRA19 DBR grid with simulated intrusion locations

2.2 Boundary Conditions

The DBR grid domain is surrounded by No Flow boundary conditions.

Some of the DBR calculations are for a drilling intrusion preceded by an earlier intrusion in either the same or a different waste panel. Prior intrusions are simulated in the Lower waste region, in the location denoted by the red dot labeled “boundary condition well” in Figure 1. The method of incorporating the prior intrusions into the DBR calculations varies by the type of intrusion. All prior intrusions are given an initial saturation of 100% at the prior intrusion location. If the prior intrusion penetrated an underlying brine pocket (E1 type intrusions), then a boundary condition well is added to the simulation, with properties that depend on the properties of the brine pocket and waste panel output by the BRAGFLO Salado model, and the amount of time that has elapsed since the prior intrusion occurred. The properties of the boundary condition are then calculated assuming steadystate conditions between the intruded repository panel and underlying brine pocket (Attachment A, Stoelzel 1996).

2.3 Initial Conditions

Volume averaged brine pressures and brine saturations are calculated during the BRAGFLO Salado simulations (Day 2019), interpolated to the DBR intrusion times in the CUTTINGS_S

code (Kicker 2019), and then used as initial conditions in the DBR simulations. The waste regions in the BRAGFLO Salado flow grid and the BRAGFLO DBR grid are each divided into three waste regions, preserving volume between the two grids, and volume-averaged brine pressure and saturations are transferred from corresponding regions in the Salado grid to the DBR grid.

Figure 2 illustrates the method used to transfer initial conditions in the waste for the CRA19 PA, which is unchanged from the CRA-2014 DBR runs. The volume averaged pressure and saturation from the three waste-filled regions in the BRAGFLO grid (WAS_AREA, SRoR, NRoR) at the time of the intrusion are used as the initial pressure and saturation for the three waste regions in the DBR grid (Lower, Middle, and Upper, respectively). The pressure and saturation are allowed to change during the DBR calculations.

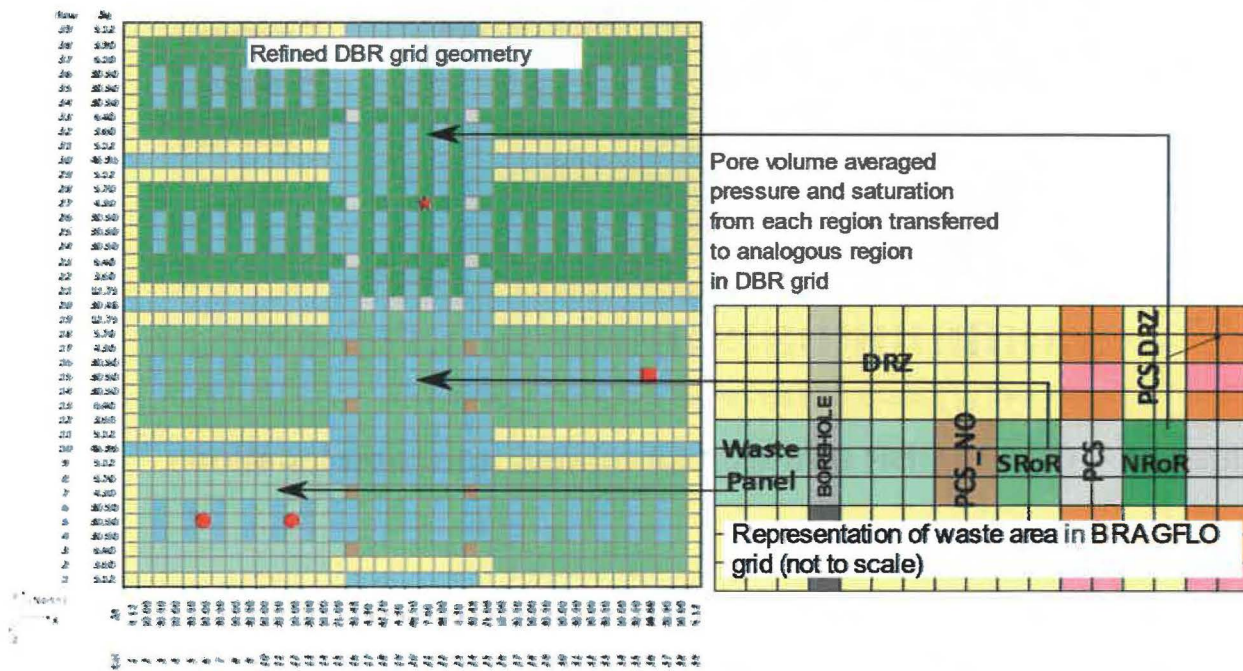


Figure 2 – Regions used to transfer initial pressure and saturation from the BRAGFLO Salado grid to the DBR grid

3.0 DBR METHODOLOGY

This section provides an overview of the methodology used in the CRA-2019 PA DBR calculations, including the modeled scenarios and run control narrative.

3.1 Modeled Scenarios

In performing DBR calculations, five of the BRAGLFO Salado model scenarios S1-BF to S5-BF are used to set the initial conditions in the DBR calculations at the time of intrusion. The five BRAGFLO Salado scenarios capture the long-term behavior of the repository under three different conditions: undisturbed, intersected by a borehole that continues down to a hypothetical pressurized brine reservoir below the repository (E1), and intersected by a borehole that terminates at the repository horizon (E2) (Day, 2019). DBR calculations map the resulting BRAGFLO pressure and saturation conditions at a suite of intrusion times onto the DBR model grid, and simulate flow to the intrusion. The scenarios and intrusion times used for the CRA-2019 PA are the same as those used for the CRA-2014 PA (Table 3).

Table 3 – DBR scenarios

Scenario	Description
S1-DBR	Initially undisturbed repository (i.e., E0 conditions). Intrusion into lower, middle, or upper waste panel at 100; 350; 1,000; 3,000; 5,000; and 10,000 years: 18 combinations.
S2-DBR	Initial E1 intrusion at 350 years followed by a second intrusion into the same, adjacent, or nonadjacent waste panel at 550; 750; 2,000; 4,000; and 10,000 years: 15 combinations.
S3-DBR	Initial E1 intrusion at 1,000 years followed by a second intrusion into the same, adjacent, or nonadjacent waste panel at 1,200; 1,400; 3,000; 5,000; and 10,000 years: 15 combinations.
S4-DBR	Initial E2 intrusion at 350 years followed by a second intrusion into the same, adjacent, or nonadjacent waste panel at 550; 750; 2,000; 4,000; and 10,000 years: 15 combinations.
S5-DBR	Initial E2 intrusion at 1,000 years followed by a second intrusion into the same, adjacent, or nonadjacent waste panel at 1,200; 1,400; 3,000; 5,000; and 10,000 years: 15 combinations.

3.2 Code Execution and Run Control

A flow diagram that illustrates the execution order for the DBR model is provided in Figure 3. A full description of the run control for the CRA19 analysis, including names and locations of input and output files, can be found in Long (2019). As outlined in AP-181 (Zeitler 2019a), in cases where comparisons are made to the CRA-2014 PA results, the CRA14 (Rev. 2) results from the

4.0 RESULTS

The DBR calculation results for the CRA-2019 PA are presented in this section and compared to results from the CRA-2014 PA. The analysis of the CRA-2014 DBR results is described in Malama (2013) and will only be summarized herein as appropriate. Unless otherwise noted, results are summarized from all three replicates and 100 vectors.

Results from all scenarios are summarized below. Results are then further examined for scenarios S1-DBR, S2-DBR, and S4-DBR. Results from S3-DBR and S5-DBR are not examined individually because the only difference between them and S2-DBR and S4-DBR, respectively, is in the timing of drilling intrusions.

Summary statistics and plots were generated with Python, an open-source software package. The average DBR volume is calculated by the sum of DBR volumes divided by the total number of simulations. The DBR volume data were obtained from the output variable BRIN_REL which is calculated in the ALGEBRACDB post-processing step, and tabulated with SUMMARIZE (Figure 3). For consistency with previous analyses, in calculating average non-zero DBR volumes and rates, non-zero volumes are defined as volumes that are greater than 10^{-7} m^3 . Tabulated results are rounded to two decimal places.

Results are also presented in boxplots of the DBR volumes, which graphically depict the distribution of the data by drawing boxes around the 25th and 75th percentiles of the distribution with a bisecting line at the median. The box whiskers extend out from the box an additional $1.5 \cdot (Q_{75} - Q_{25})$ or to the full range of the data, whichever is closer to the median. All datapoints used to derive the boxplot are also plotted on top of the boxplot for visualization of any outliers. Note that intrusion time is treated categorically when used as an axis on the boxplots in this section.

4.1 Summary

Relative to CRA-2014, DBR events increased in both mean magnitude and frequency, resulting in increases to the overall mean DBR volume (Table 4). Releases of all magnitude increased in frequency (Figure 4), and maximum DBR volumes are also higher (seen in the outliers of Figure 5). Despite the increases, only 18% of modeled intrusions produce nonzero DBRs, and less than 15% of modeled intrusions produce DBR events greater than 1.00 m^3 .

While mean DBR volumes increased in all scenarios, the increases were most substantial in S2-DBR and S3-DBR. Releases from scenarios S2-DBR and S3-DBR had already represented the majority of total release volume (together 93.4% in CRA-2014), and with the increases now represent an even greater proportion (96.4% in CRA-2019). These results show that the majority of the non-zero DBR volumes occur when there is a previous E1 intrusion, as has been observed previously (Clayton et al., 2010; Pasch and Camphouse, 2011, and Malama, 2013).

Lower intrusions continue to produce the largest average release volumes, but relatively larger increases to the average Middle release volumes result in Middle intrusions representing a greater proportion of the total release volumes (from 3.0% in CRA-2014, 33.6% in CRA-2019). Releases from the upper location slightly decreased, both in frequency and magnitude, but because they play such a minor role in the total releases, the difference is not impactful.

Table 4 – DBR volume summary

Intrusion	Mean Brine Released (m ³)			Nonzero Release Rate			Mean Non-Zero (m ³)		
	CRA14	CRA19	Change	CRA14	CRA19	Change	CRA14	CRA19	Change
S1-DBR	0.15	0.26	0.10	4%	3%	-2%	3.80	10.11	6.31
Lower	0.37	0.70	0.33	7%	5%	-1%	5.56	12.87	7.31
Middle	0.08	0.07	-0.02	3%	1%	-2%	2.54	5.62	3.08
Upper	0.01	0.00	-0.01	2%	1%	-1%	0.49	0.30	-0.19
S2-DBR	3.31	8.29	4.97	25%	47%	22%	13.12	17.55	4.43
Lower	9.84	15.64	5.80	70%	74%	4%	14.10	21.27	7.18
Middle	0.09	9.21	9.12	4%	66%	62%	2.63	13.94	11.31
Upper	0.01	0.00	-0.01	2%	2%	0%	0.43	0.15	-0.28
S3-DBR	2.14	5.23	3.09	22%	40%	19%	9.79	12.94	3.15
Lower	6.32	10.83	4.52	59%	67%	8%	10.75	16.27	5.52
Middle	0.10	4.86	4.76	4%	53%	49%	2.47	9.19	6.72
Upper	0.01	0.00	-0.01	3%	2%	-1%	0.44	0.22	-0.22
S4-DBR	0.09	0.07	-0.02	2%	1%	-1%	3.82	7.14	3.31
Lower	0.19	0.22	0.04	3%	2%	0%	6.85	9.83	2.98
Middle	0.07	0.00	-0.07	2%	0%	-2%	3.15	0.18	-2.97
Upper	0.01	0.00	-0.01	2%	0%	-2%	0.48	0.01	-0.47
S5-DBR	0.11	0.12	0.02	3%	2%	-1%	3.73	7.70	3.97
Lower	0.22	0.36	0.14	4%	2%	-2%	5.87	10.10	4.23
Middle	0.09	0.01	-0.08	3%	0%	-2%	3.43	1.38	-2.05
Upper	0.01	0.00	-0.01	2%	0%	-2%	0.49	0.01	-0.48
Lower	3.27	5.37	2.09	28%	29%	2%	11.89	18.29	6.41
Middle	0.09	2.72	2.63	3%	23%	20%	2.77	11.65	8.88
Upper	0.01	0.00	-0.01	2%	1%	-1%	0.47	0.18	-0.29
ALL	1.12	2.70	1.57	11%	18%	7%	10.19	15.02	4.83

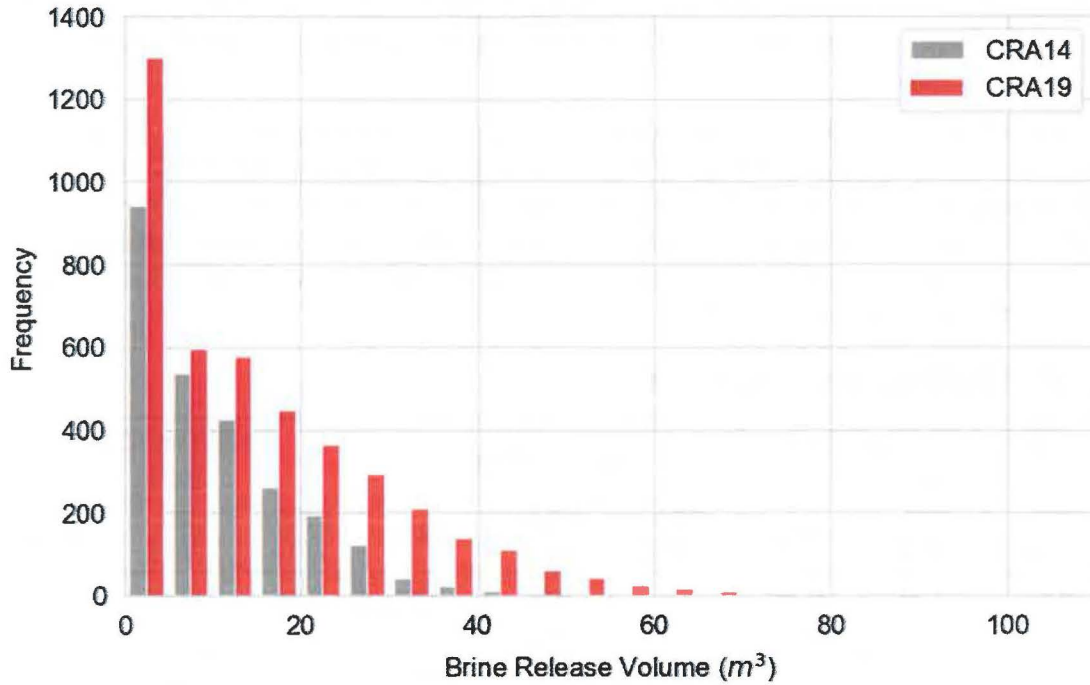


Figure 4 – Release volume frequency, all intrusions

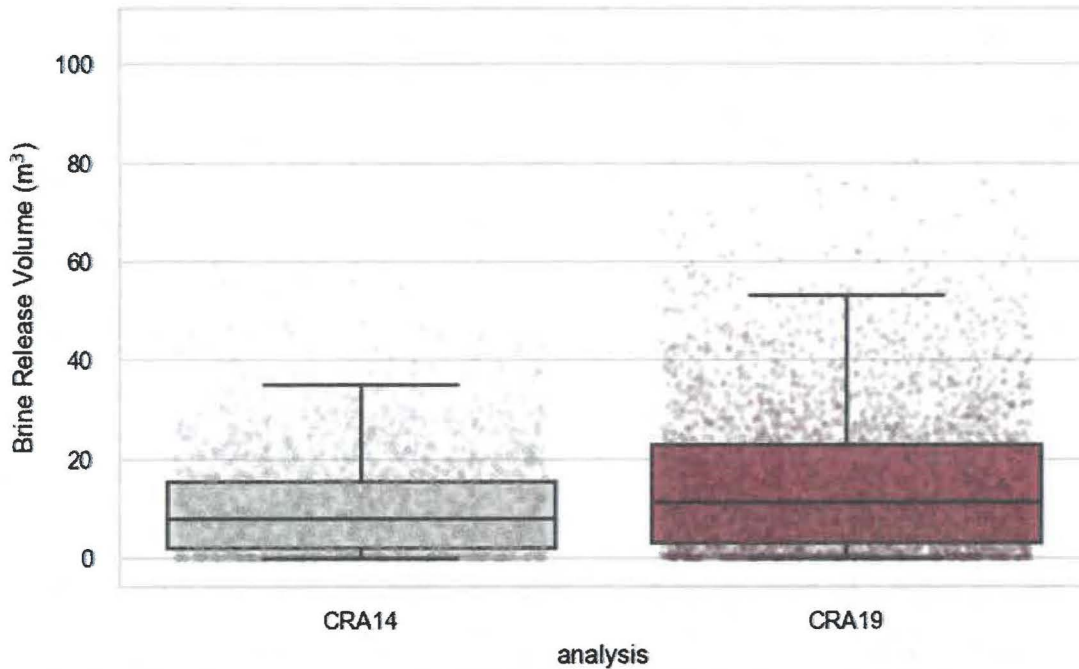


Figure 5 – Release volume boxplots, all non-zero events

4.2 S1-DBR

CRA-2019 S1-DBR release volumes are summarized in Table 5, below, with CRA-2014 values for comparison. Release volumes for all S1-DBR intrusions are plotted in Figure 6, grouped by intrusion location and time.

Relative to CRA-2014, CRA-2019 S1-DBR average release rates are slightly lower, while average non-zero release volumes are slightly higher, with the net result being a slight increase in average brine release of 0.15 to 0.26 m³. Intrusions into the lower region account for the majority of the difference, increasing from 0.37 to 0.70 m³, with greater differences at later times. Average non-zero releases are increased at all times in the lower and middle locations. Upper intrusion release volumes remain low.

Table 5 – S1-DBR volume summary

Loc Time	Mean Brine Released (m ³)			Release Rate			Mean Non-Zero (m ³)		
	CRA- 2014	CRA- 2019	Chg	CRA- 2014	CRA- 2019	Chg	CRA- 2014	CRA- 2019	Chg
L	0.37	0.70	0.33	7%	5%	-1%	5.56	12.87	7.31
100	0.00	0.00	0.00	0%	0%	0%	--	--	--
350	0.00	0.00	0.00	0%	0%	0%	--	--	--
1,000	0.00	0.11	0.11	0%	2%	2%	--	5.64	5.64
3,000	0.53	1.26	0.73	8%	9%	1%	6.38	14.05	7.67
5,000	0.95	1.39	0.44	14%	10%	-4%	6.66	13.95	7.29
10,000	0.74	1.43	0.69	17%	12%	-6%	4.26	12.28	8.02
M	0.08	0.07	-0.02	3%	1%	-2%	2.54	5.62	3.08
100	0.00	0.00	0.00	0%	0%	0%	--	--	--
350	0.00	0.00	0.00	0%	0%	0%	--	--	--
1,000	0.00	0.06	0.06	0%	1%	1%	--	9.51	9.51
3,000	0.16	0.16	0.00	4%	2%	-2%	3.59	6.73	3.13
5,000	0.23	0.13	-0.09	7%	2%	-6%	3.10	8.05	4.95
10,000	0.11	0.04	-0.07	8%	2%	-5%	1.41	1.67	0.25
U	0.01	0.00	-0.01	2%	1%	-1%	0.49	0.30	-0.19
100	0.00	0.00	0.00	0%	0%	0%	--	--	--
350	0.00	0.00	0.00	0%	0%	0%	--	--	--
1,000	0.00	0.00	0.00	0%	0%	0%	--	--	--
3,000	0.03	0.01	-0.02	1%	2%	1%	2.25	0.46	-1.79
5,000	0.02	0.01	-0.02	5%	2%	-3%	0.46	0.33	-0.13
10,000	0.02	0.00	-0.01	8%	2%	-6%	0.20	0.10	-0.10
S1-DBR	0.15	0.26	0.10	4%	3%	-2%	3.80	10.11	6.31

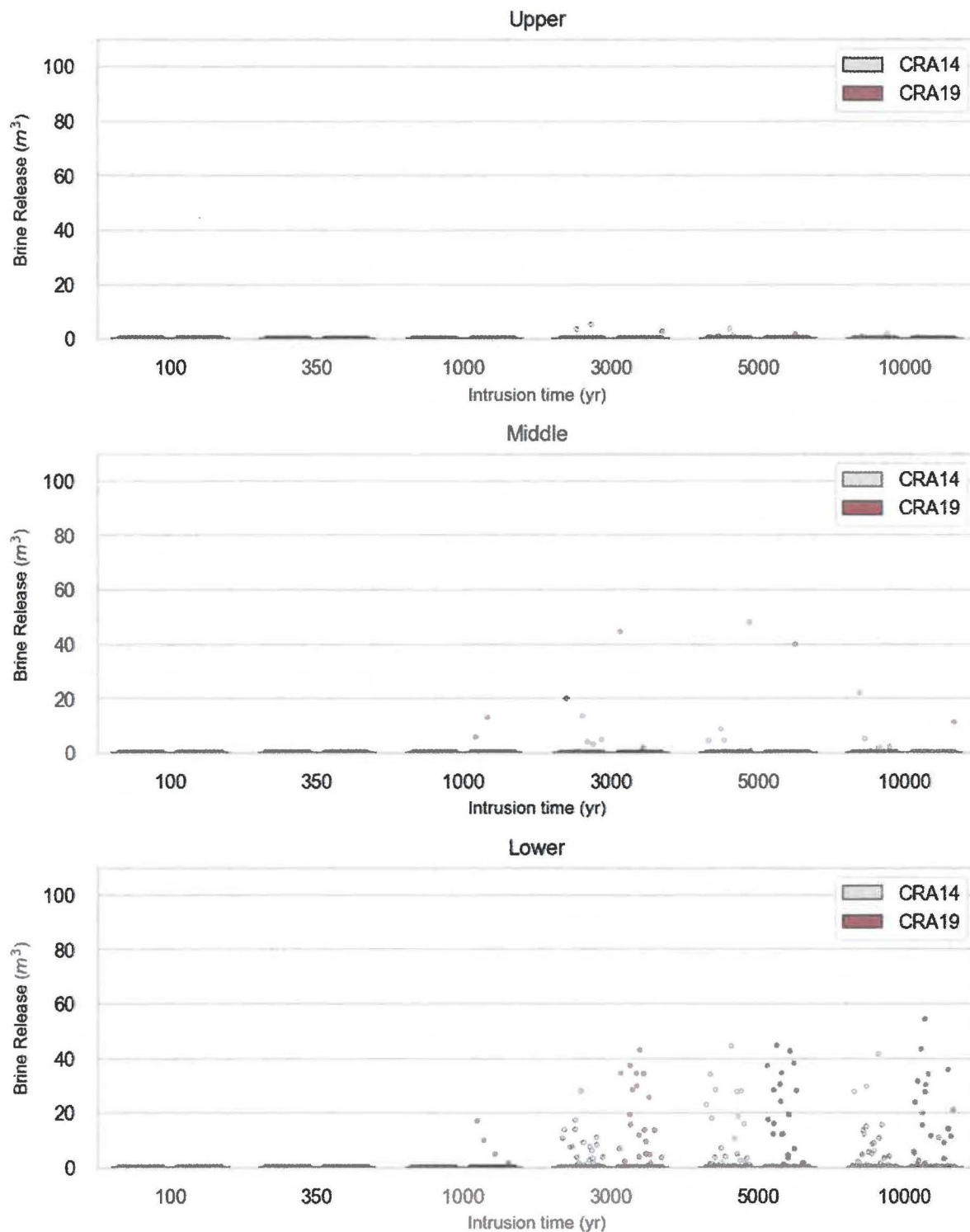


Figure 6 – S1-DBR release volume boxplots, all intrusions

4.3 S2-DBR

CRA-2019 S2-DBR release volumes are summarized in Table 6, below, with CRA-2014 values shown for comparison. Release volumes for all S2-DBR intrusions are plotted in Figure 7, grouped by intrusion location and time.

Average S2-DBR volumes are significantly higher in CRA-2019 than they were in CRA-2014. Release events increased substantially in both frequency and magnitude in the lower and middle intrusions. Release volumes are still larger and more frequent in the lower intrusions, but the increases were more substantial from the middle intrusions, and represent a much greater relative increase.

Scenario 2 maximum release volumes are higher in CRA-2019 than CRA-2014, with the boxplots showing a more skewed left distribution with higher maxima (Figure 7) in the lower and middle intrusion locations. Upper intrusion release volumes remain low.

Table 6 – S2-DBR volume summary

Loc Time	Mean Brine Released (m ³)			Release Rate			Mean Non-Zero (m ³)		
	CRA- 2014	CRA- 2019	Chg	CRA- 2014	CRA- 2019	Chg	CRA- 2014	CRA- 2019	Chg
L	9.84	15.64	5.80	70%	74%	4%	14.10	21.27	7.18
550	11.14	9.45	-1.69	94%	82%	-11%	11.89	11.48	-0.42
750	13.48	15.87	2.39	95%	91%	-5%	14.14	17.50	3.36
2000	11.48	20.31	8.83	71%	76%	4%	16.09	26.83	10.75
4000	8.37	18.19	9.82	55%	64%	9%	15.21	28.27	13.05
10000	4.73	14.41	9.67	34%	55%	21%	14.06	26.35	12.29
M	0.09	9.21	9.12	4%	66%	62%	2.63	13.94	11.31
550	0.00	10.86	10.86	0%	81%	81%	--	13.40	13.40
750	0.00	13.13	13.13	0%	89%	89%	--	14.70	14.70
2000	0.09	12.18	12.09	2%	70%	68%	5.20	17.48	12.28
4000	0.25	7.23	6.98	8%	53%	45%	3.26	13.64	10.37
10000	0.14	2.66	2.52	9%	37%	29%	1.58	7.12	5.54
U	0.01	0.00	-0.01	2%	2%	0%	0.43	0.15	-0.28
550	0.00	0.00	0.00	0%	0%	0%	--	--	--
750	0.00	0.00	0.00	0%	0%	0%	--	--	--
2000	0.01	0.00	0.00	0%	3%	3%	2.26	0.09	-2.17
4000	0.03	0.01	-0.02	5%	5%	0%	0.67	0.25	-0.42
10000	0.01	0.00	-0.01	7%	3%	-4%	0.19	0.04	-0.15
S2-DBR	3.31	8.29	4.97	25%	47%	22%	13.12	17.55	4.43

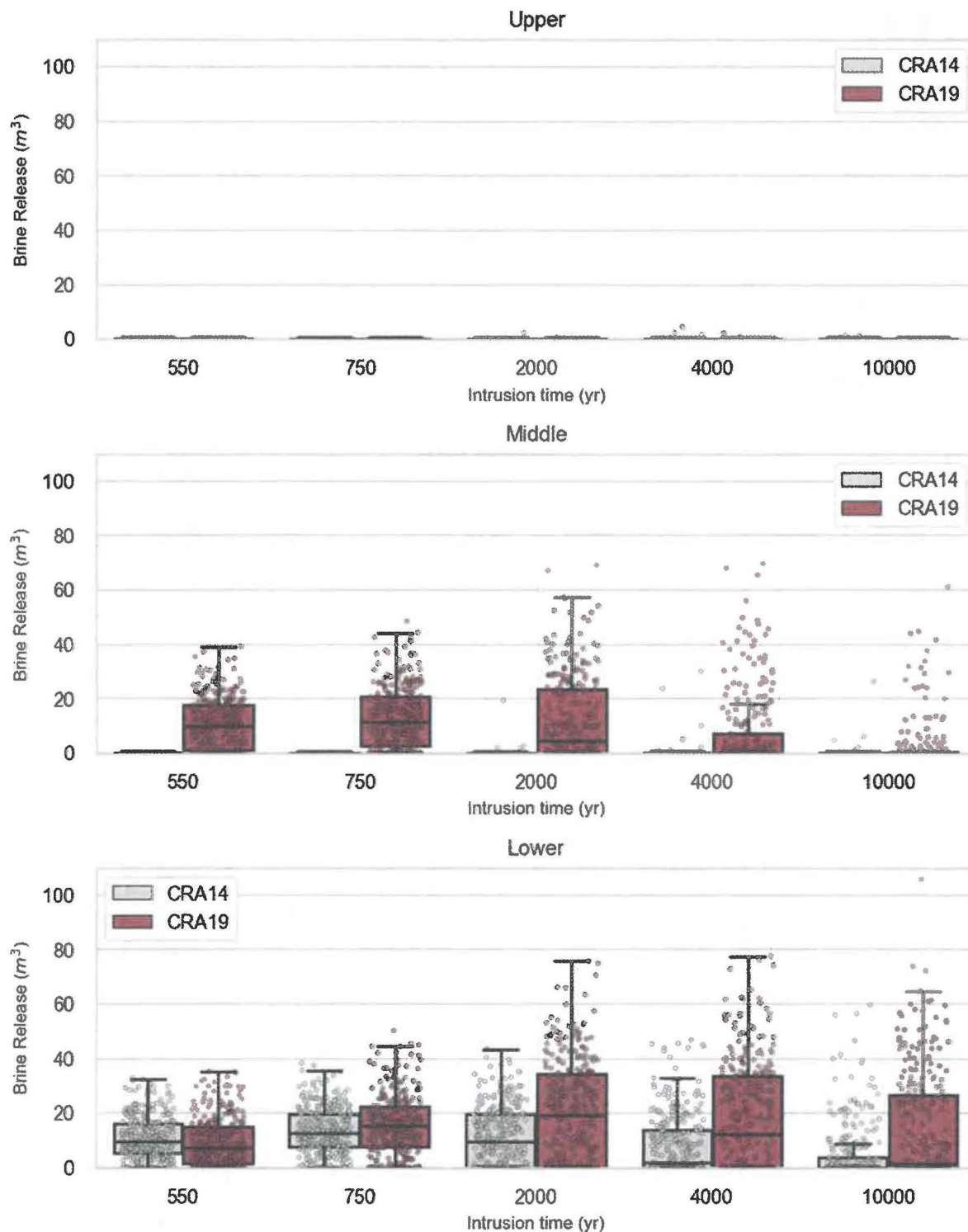


Figure 7 – S2-DBR release volumes, all intrusions

4.4 S4-DBR

CRA-2019 S4-DBR release volumes are summarized in Table 7, below, with CRA-2014 values for comparison. Release volumes for all S4-DBR intrusions are plotted in Figure 8, grouped by intrusion location and time.

CRA-2019 S4-DBR volumes are slightly lower in than they were in CRA-2014. Frequencies are down in all intrusion locations, while average nonzero releases increased in the lower intrusions and decreased in the middle and upper intrusions. Mean volumes decreased in the lower intrusions frequency and magnitude. The increases in the middle intrusions are consistent at all intrusion times, though most pronounced at early times. Releases are highest at later times. Release volumes from upper intrusion release volumes remain low.

Table 7 – S4-DBR volume summary

Loc Time	Mean Brine Released (m ³)			Release Rate			Mean Non-Zero (m ³)		
	CRA- 2014	CRA- 2019	Chg	CRA- 2014	CRA- 2019	Chg	CRA- 2014	CRA- 2019	Chg
L	0.19	0.22	0.04	3%	2%	0%	6.85	9.83	2.98
550	0.00	0.00	0.00	0%	0%	0%	--	--	--
750	0.00	0.00	0.00	0%	0%	0%	--	--	--
2000	0.08	0.25	0.17	1%	2%	1%	6.17	10.75	4.57
4000	0.38	0.42	0.04	5%	5%	0%	8.17	8.93	0.76
10000	0.47	0.45	-0.03	8%	4%	-3%	6.16	10.30	4.15
M	0.07	0.00	-0.07	2%	0%	-2%	3.15	0.18	-2.97
550	0.00	0.00	0.00	0%	0%	0%	--	--	--
750	0.00	0.00	0.00	0%	0%	0%	--	--	--
2000	0.05	0.00	-0.05	1%	0%	-1%	4.05	0.00	-4.05
4000	0.17	0.00	-0.17	5%	1%	-4%	3.46	0.43	-3.04
10000	0.14	0.00	-0.14	5%	1%	-4%	2.63	0.08	-2.55
U	0.01	0.00	-0.01	2%	0%	-2%	0.48	0.01	-0.47
550	0.00	0.00	0.00	0%	0%	0%	--	--	--
750	0.00	0.00	0.00	0%	0%	0%	--	--	--
2000	0.01	0.00	-0.01	0%	0%	0%	2.06	--	-2.06
4000	0.03	0.00	-0.03	4%	2%	-2%	0.76	0.00	-0.75
10000	0.01	0.00	-0.01	6%	1%	-5%	0.19	0.04	-0.16
S4-DBR	0.09	0.07	-0.02	2%	1%	-1%	3.82	7.14	3.31

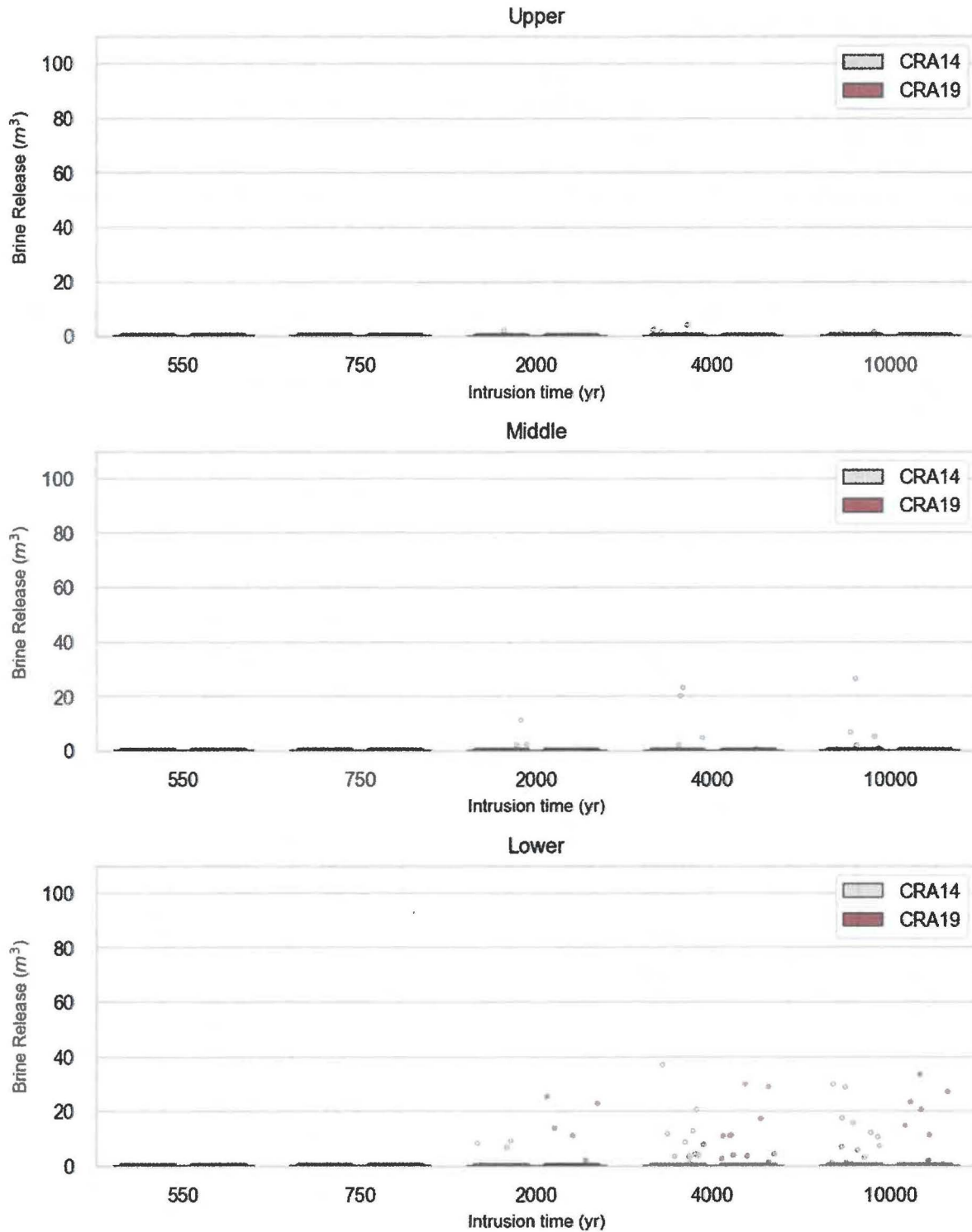


Figure 8 – S4-DBR releases volumes, all intrusions

4.5 Maximum Releases

The 10 highest DBR release volumes are significantly larger in CRA-2019 than they were in CRA-2014, encountering both higher average brine pressures and higher average brine saturations (Table 8). Note that the absolute largest releases volumes do not necessarily come from simulations with the highest saturation or pressure, in either analysis. All 10 of the highest release volumes simulated in CRA-2019 all came from lower intrusions, while the 6th highest release volume from the CRA-2014 analysis came from the middle panel.

Table 8 – Largest DBR volumes by analysis

Analysis	Rank	Rep	Scn	Time	Vec	Loc	Release (m ³)	Pressure (MPa)	Saturation (-)
CRA19	1	3	2	10000	99	L	105.79	17.20	0.90
CRA19	2	3	3	10000	99	L	80.46	16.80	0.84
CRA19	3	3	2	4000	99	L	77.44	16.60	0.96
CRA19	4	2	2	4000	1	L	76.07	14.40	0.99
CRA19	5	3	2	2000	94	L	75.67	16.10	0.97
CRA19	6	3	2	2000	81	L	74.78	15.60	0.82
CRA19	7	3	2	4000	94	L	74.05	15.80	0.97
CRA19	8	2	2	10000	78	L	73.82	14.60	0.99
CRA19	9	2	2	4000	78	L	72.72	14.60	0.85
CRA19	10	3	2	10000	15	L	72.13	15.70	1.00
						Average	78.29	15.74	0.93
CRA14	1	2	2	10000	76	L	59.57	15.00	0.69
CRA14	2	2	2	10000	1	L	56.38	13.40	0.99
CRA14	3	3	3	10000	99	L	56.23	15.80	0.96
CRA14	4	3	2	10000	99	L	55.85	15.80	0.96
CRA14	5	2	3	10000	1	L	54.6	13.30	0.89
CRA14	6	2	1	5000	63	M	47.96	11.90	0.69
CRA14	7	2	3	5000	76	L	47.57	14.40	0.84
CRA14	8	2	2	4000	76	L	46.74	14.50	0.97
CRA14	9	1	2	10000	87	L	46.41	12.70	0.92
CRA14	10	1	2	4000	65	L	45.47	15.70	0.93
						Average	51.68	14.25	0.88

5.0 DRIVERS AND CORRELATIONS

In this section, initial brine pressure and saturation as well as the cross-sectional area of the intruding borehole are summarized and compared for the CRA14 PA and CRA19 PA DBR analyses. Volume-averaged brine pressure and brine saturation in the intruded panel have been previously identified as the two most important variables that control DBR volumes (Clayton 2008). Borehole area was not previously identified as a strongly controlling variable, but because its values have been affected by changes in CUTTINGS_S input, it is included in the summary. For discussion of the modeling setup that produced the input conditions, and more comprehensive analyses of those results, see Day (2019) and Kicker (2019).

Sensitivity of DBR volumes to initial brine pressure and saturation conditions and borehole areas will also be qualitatively examined to determine what if any impact the changes to the model design and initialization may have had on brine release sensitivity to the controlling variables.

Pressure, saturation, and borehole size values were extracted from the ALGEBRACDB output files generated as a preprocessing step for the DBR input (Figure 3). Pressure and saturation values were extracted from the intruded region, and so represent the pressure and saturation conditions encountered by the intrusion. Borehole area values represent the cross sectional areas of the intruding boreholes; however, because borehole area is not dependant on pressure or saturation conditions, borehole area is independent of intrusion location.

Scenarios S2-DBR and S3-DBR both have significant DBR volumes (Section 4.1), but due to the similarity between them, only scenario S2-DBR is discussed in the presentation of initial conditions and in the sensitivity analyses, consistent with previous reports (e.g., Stoelzel 1996).

Because lower intrusions had previously produced the majority of DBRs, they were the only intrusions examined in the sensitivity studies of previous DBR analysis packages (e.g., Stoelzel 1996), but because Middle intrusions now represent a significant portion of the non-zero DBRs, they are included in this analysis below.

5.1 Initial Conditions Summary

CRA19 DBR mean initial conditions are presented in Table 9 with CRA14 values for comparison. Boxplots of initial pressure (Figure 9) and saturation (Figure 10) are also shown below with all intrusion values included in the distributions.

Average CRA19 initial brine pressure have risen relative to CRA14 in Scenario S2-DBR in both the lower and middle intrusion locations. In the lower intrusion location initial pressures at early times are slightly lower in CRA-2019 than CRA14, but by the intrusion at time 2000 years have become higher, and continue to rise away from CRA-2014 values for all intrusion times thereafter. The distribution of initial pressures also span a wider range in CRA-2019, with a wider range captured by the middle quantiles and more extreme upper and lower outliers than in CRA-2014 (Figure 9). In both analyses, most lower intrusions encounter pressure conditions above the 6 MPa threshold for a DBR. Average initial pressure in the middle intrusion is substantially higher in CRA-2019 relative to CRA-2014. The distribution of pressure in the middle location has shifted up, such that the median values are above all but the outliers of the

CRA-2014 values. This shift has resulted in more CRA-2019 initial pressure values above the 6 MPa threshold for a DBR event than there were in CRA-2014.

Brine saturations show two distinct trends in the lower and middle locations. In the lower location, brine saturation is decreased slightly relative to CRA-2014, with a slightly decreased median value and lower outlier values (Figure 10). Brine saturation in the lower location in both analyses is high though, and the difference between them is on average relatively small. Average saturation in the middle location is much higher in CRA-2019 than CRA-2014, and the entire distribution of values has shifted up and shows greater spread about the median. The average saturation values are lower at later intrusion times, but remain much higher than the CRA-2014 values, and the distribution becomes wide enough to span nearly the entire range of possible values.

In general, the initial conditions of the middle location are more similar to the lower location in CRA-2019 than they had been in CRA-2014. In CRA-2014 the pressures of the middle location are on average more than 8 MPa below those of the lower location in the 550-year intrusions, and are still on average more than 1.5 MPa below those of the lower location in the 10,000-year intrusions. In CRA-2019, on the other hand, pressures in the middle location remain within 0.5 MPa of the lower location at all simulated intrusion times. Saturation values are similarly closer in the lower and middle locations in CRA-2019 than they are in CRA-2014. In CRA-2014 the saturations of the middle location are on average 0.80 below those of the lower location in the 550-year intrusions, and actually become even further apart at late-time intrusions. In CRA-2019, saturations in the middle location remain within 0.10 to 0.31 of the lower location at all simulated intrusion times.

Table 9 – S2-DBR mean initial conditions, lower and middle locations

Location Time	Brine Pressure (MPa)			Brine Saturation (-)		
	CRA-2014	CRA-2019	Change	CRA-2014	CRA-2019	Change
L	9.44	10.17	0.74	0.91	0.87	-0.04
550	9.76	9.17	-0.59	0.92	0.89	-0.03
750	10.40	10.18	-0.22	0.91	0.90	-0.01
2000	9.99	10.94	0.95	0.90	0.87	-0.03
4000	9.02	10.59	1.58	0.90	0.84	-0.06
10000	8.02	9.99	1.97	0.91	0.83	-0.07
M	3.59	10.14	6.55	0.10	0.67	0.56
550	1.43	9.14	7.72	0.12	0.79	0.68
750	1.80	10.14	8.34	0.12	0.78	0.66
2000	3.44	10.90	7.47	0.11	0.68	0.57
4000	4.90	10.56	5.67	0.09	0.56	0.47
10000	6.39	9.95	3.56	0.07	0.52	0.44
S2-DBR	5.39	8.85	3.46	0.37	0.53	0.16

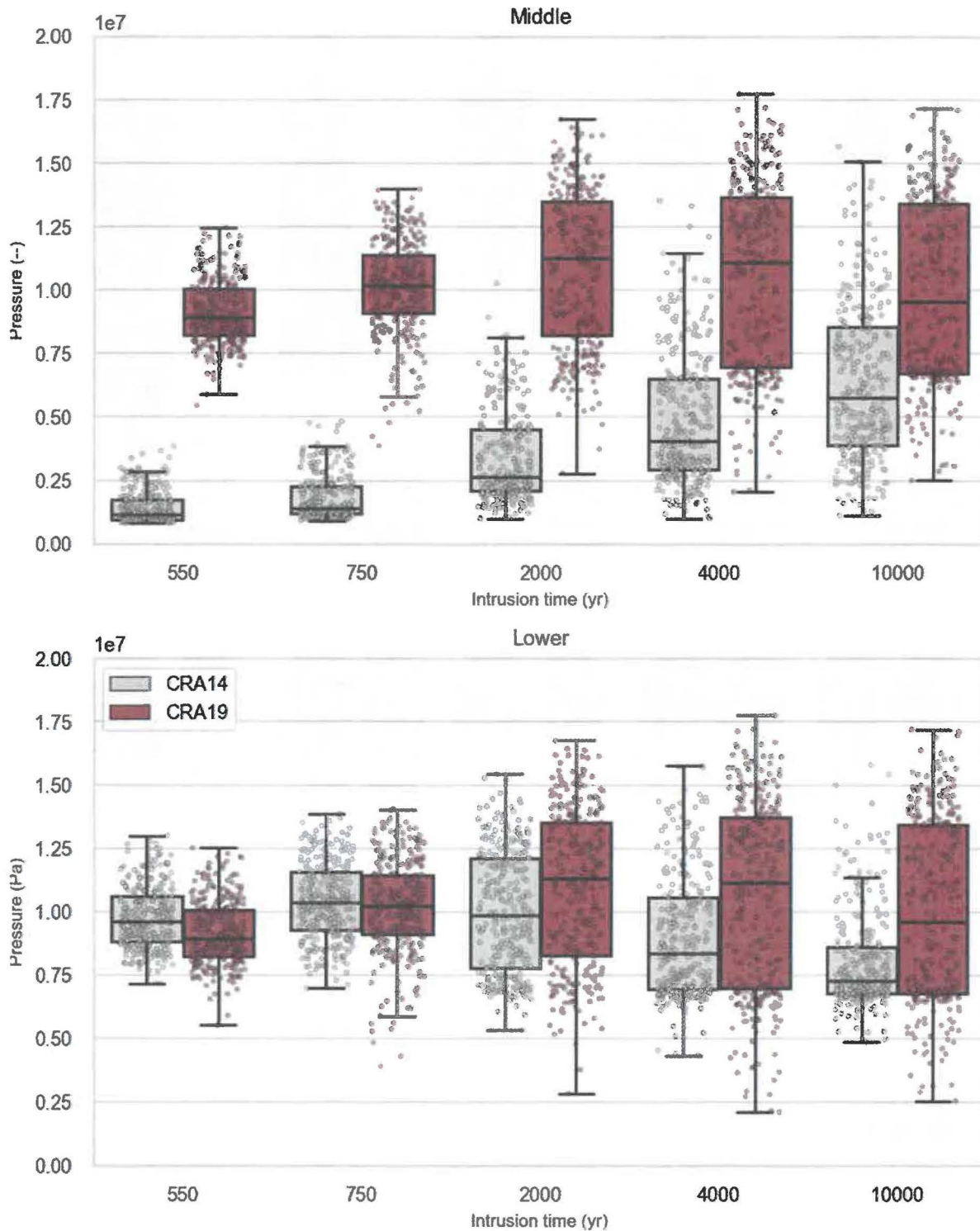


Figure 9 – S2-DBR brine pressure, all lower and middle intrusions

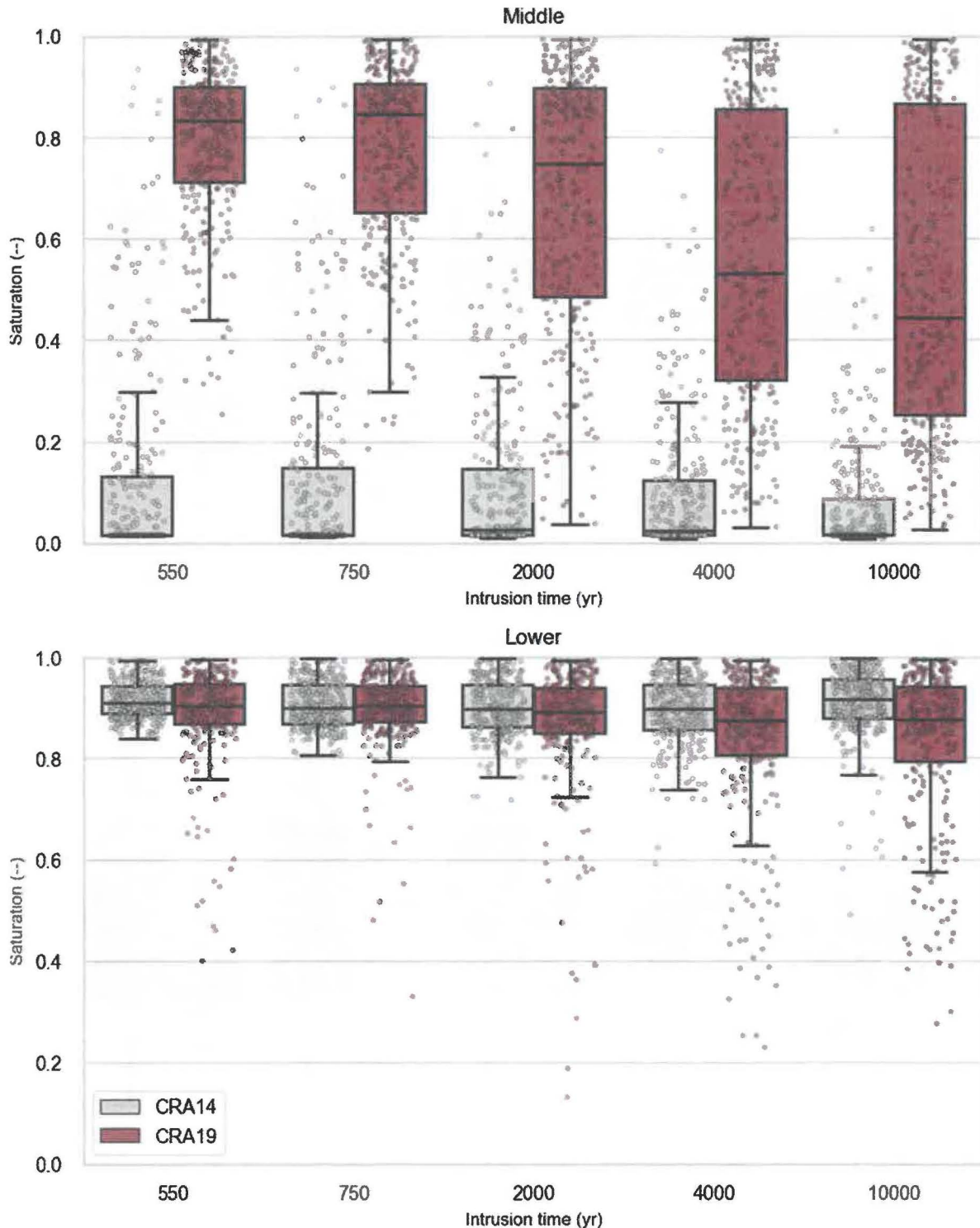


Figure 10 – S2-DBR brine saturation, all lower and middle intrusions

5.2 Sensitivity to Initial Conditions

Scatter plots were created to visualize the sensitivity of CRA-2019 DBR volume to initial panel pressure and saturation (Figure 11 and Figure 12, respectively) with CRA-2014 plotted separately for comparison. As was done in previous DBR analysis reports, saturation is plotted as mobile brine saturation, calculated as the residual brine saturation subtracted from the brine saturation (Stoelzel 1996). Regression statistics were calculated with python SciPy statistics package, and the line of best fit plotted over the data. Simulations with zero releases were not plotted or included in the regression analysis.

Each simulation was categorized into flow regimes from the ratio of relative permeabilities of brine and gas, as is done in the ALGEBRACDB preprocessing step to calculate flowing bottom hole pressure (Eqn 1 and Stoelzel 1996). Simulations were categorized as “All brine” if the gas relative permeability is zero, “Brine dominated” if the gas relative permeability is lower than the brine relative permeability, and “Gas dominated” if the gas relative permeability is higher than the brine relative permeability. Because flow regime is a function of both brine saturations and residual brine saturation, the same brine saturation can be categorized into multiple flow regimes (Figure 13).

Brine pressure has the strongest correlation with (measured by the r^2 value), and effect on (measured by the slope of the fitted curve) brine release volume when the panel is fully saturated. When the panel is under a brine dominated flow regime, the correlation and effect is slightly weaker. And when the flow regime is gas dominated, pressure has very little correlation with release volume. The same pattern is observed with both CRA-2014 and CRA-2019 results, but the slopes of the curves are higher with CRA-2019 with very slightly higher r^2 values, indicating the CRA-2019 DBR volumes are slightly more sensitive to pressure than they had been in CRA-2014.

Brine saturation appears to correlate with brine release volumes under gas dominated flow regimes, and to a lesser extent under fully saturated flow regimes; however, there does not appear to be any relationship between brine release and saturation under brine dominated flow regimes. Relative to CRA14, the correlations between DBR volume and mobile brine saturation are about the same strength, with slightly steeper trends.

Taken together, these results indicate that at low saturations, DBR intrusions are more sensitive to panel saturation than they are to pressure, but once saturation increases enough to produce a brine dominated flow regime, panel saturation becomes much less important than panel pressure. Fully saturated panels are sensitive to both panel saturation and panel pressure.

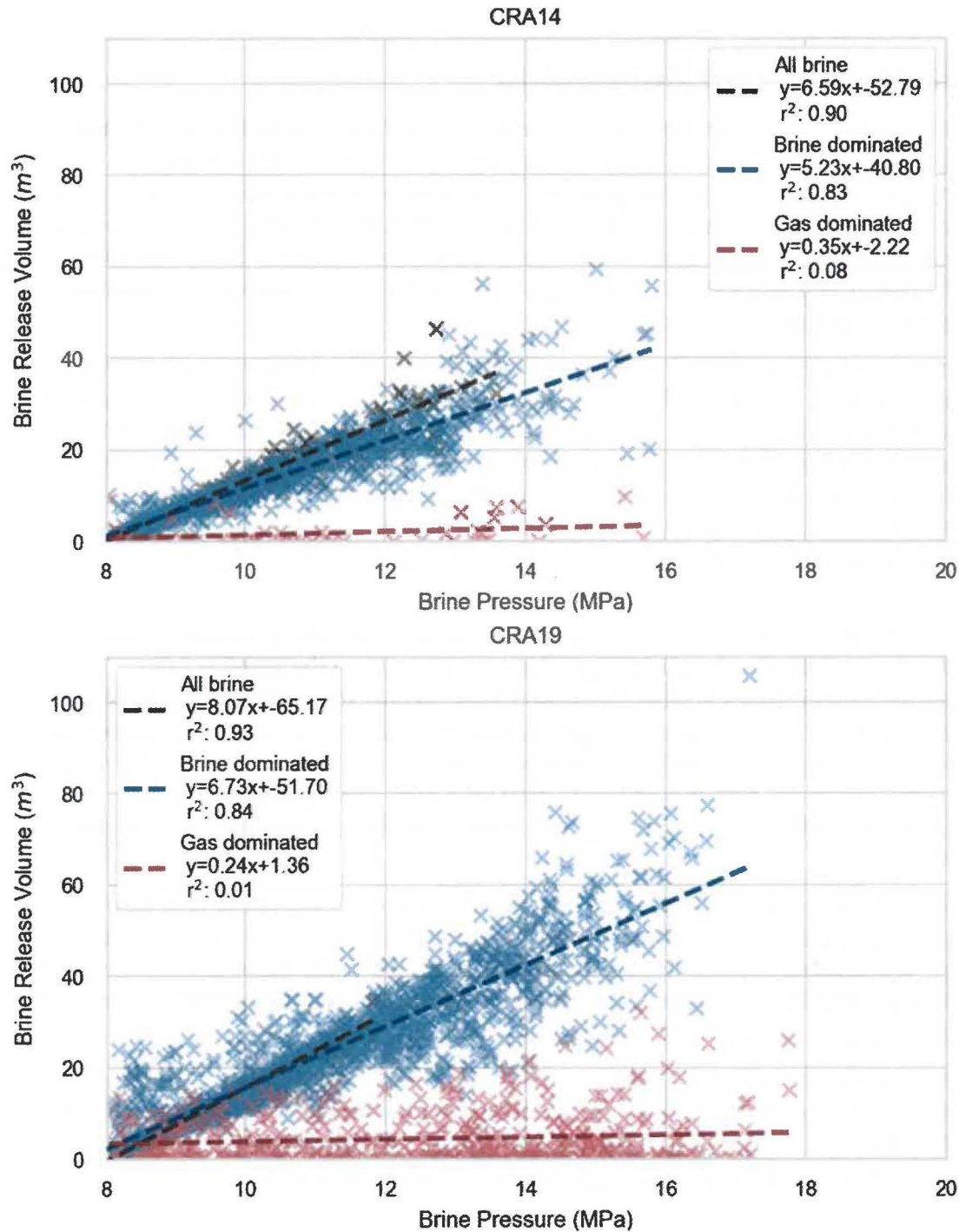


Figure 11 – S2-DBR release volume versus brine pressure, all non-zero lower and middle intrusions

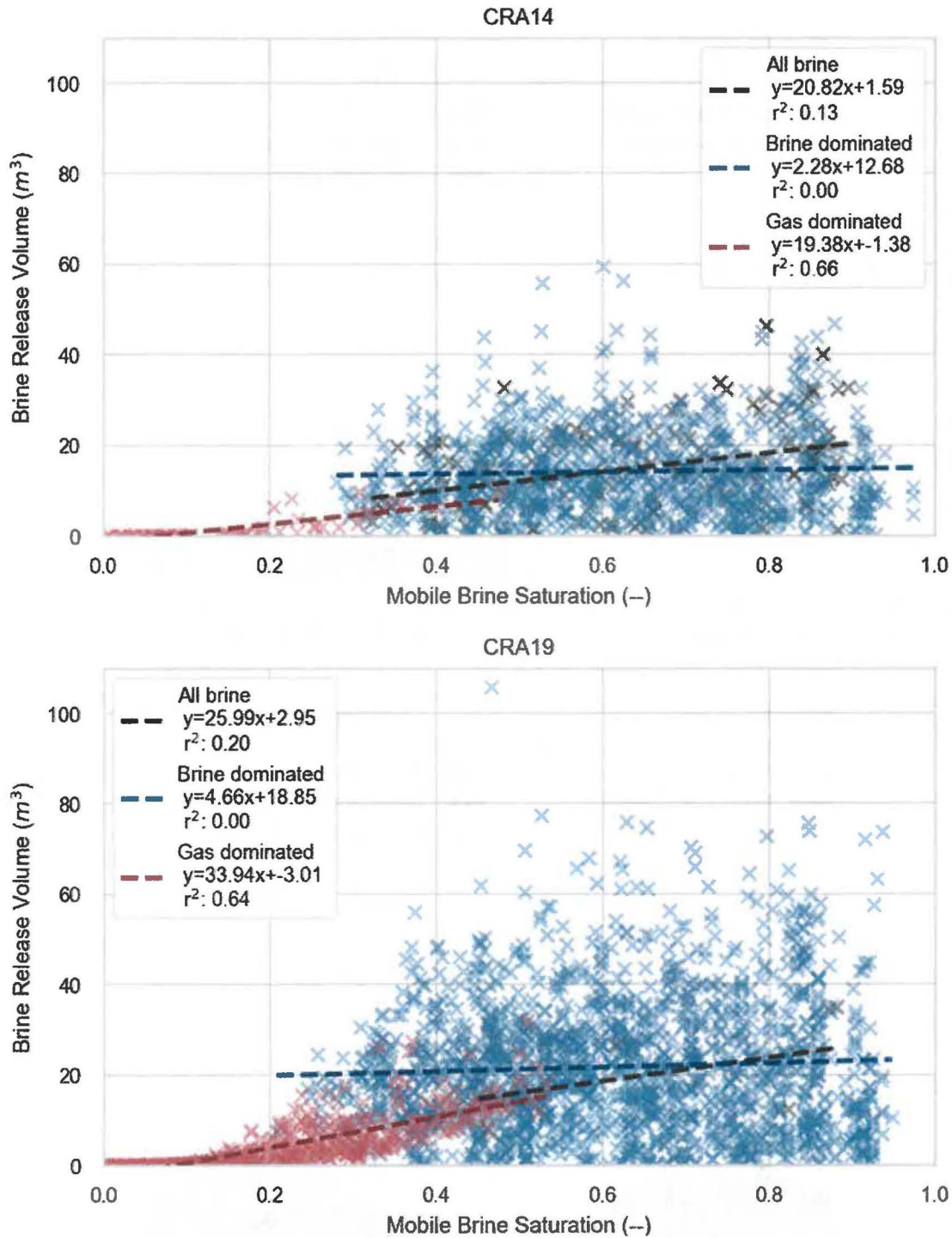


Figure 12 – S2-DBR release volume versus brine saturation, all non-zero lower and middle intrusions

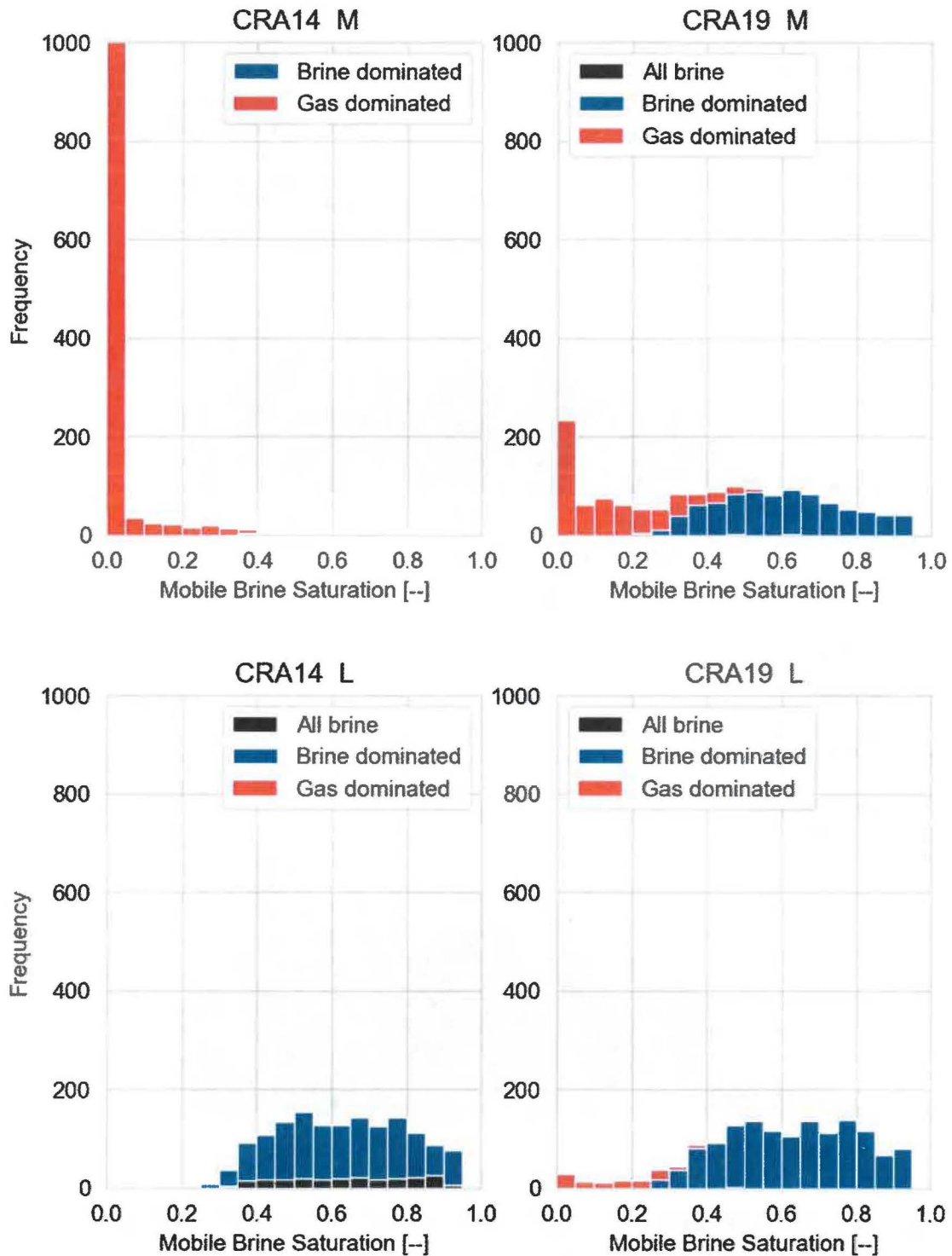


Figure 13 – Brine saturation frequency, S2-DBR all lower and middle intrusions

5.3 Borehole Size Summary

Borehole is calculated in CUTTINGS_S as a product of drill bitsize and the extent of cavings around the borehole (Kicker 2019). CRA19 has higher borehole sizes on average, both mean and median values, as well as higher maxima (Table 10 and Figure 14). The differences appear to be largest at later times.

Table 10 – S2-DBR mean borehole size

Intrusion	Borehole Area (m ²)		
	CRA-2014	CRA-2019	Change
S2-DBR	0.12	0.16	0.04
550	0.10	0.09	-0.01
750	0.13	0.13	0.00
2000	0.14	0.21	0.06
4000	0.12	0.20	0.08
10000	0.10	0.18	0.08

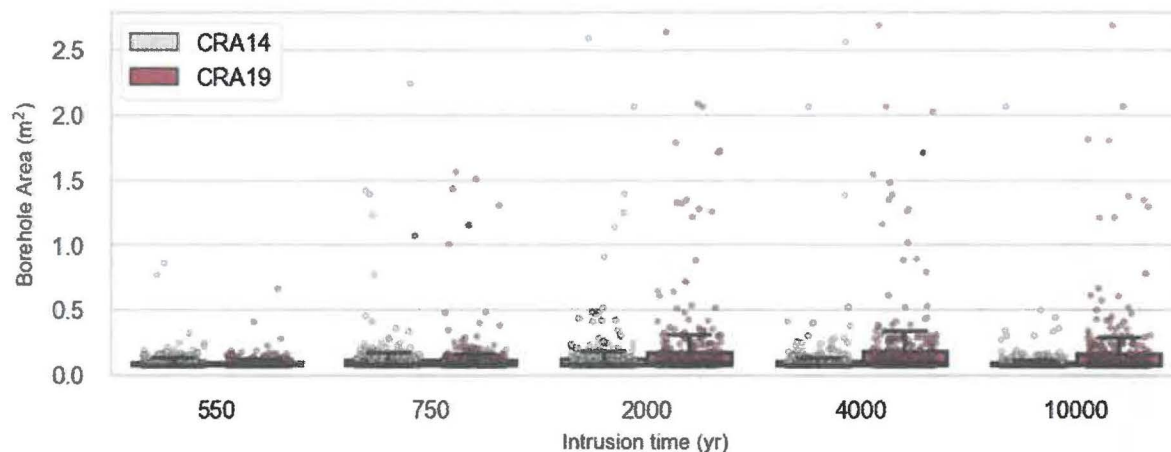


Figure 14 – S2-DBR borehole size, all intrusions

5.4 Sensitivity to Borehole Size

All else being equal, larger borehole areas should allow for greater flow, and produce larger releases (Eqn 2). However, the relationship between borehole size and release remains low and noisy even as borehole areas became larger in CRA19 (Figure 155).

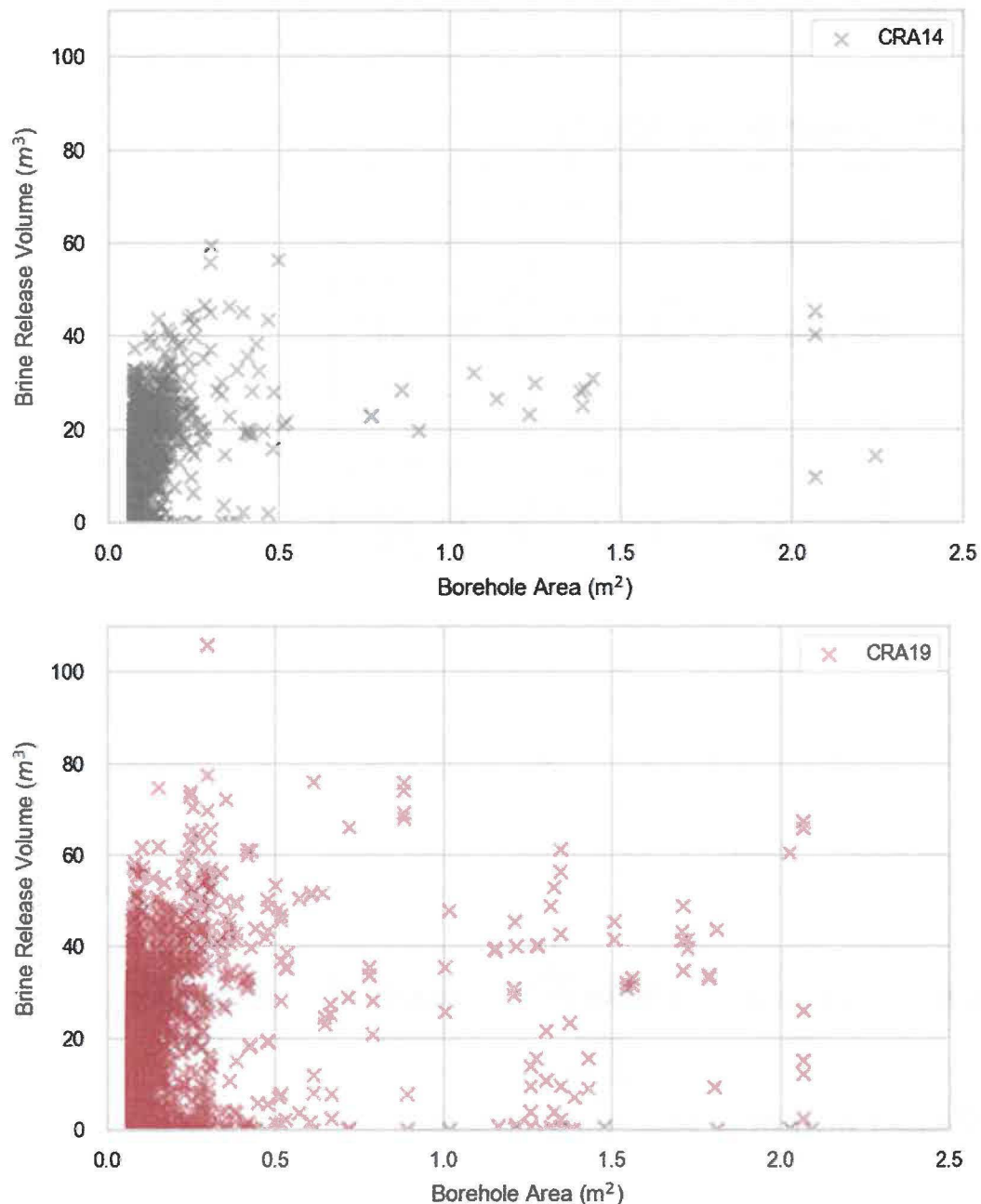


Figure 15 – Brine release versus borehole area, S2-DBR

6.0 SUMMARY

Changes incorporated into the CRA-2019 PA include planned changes as well as parameter and implementation changes. Of the changes delineated in Section 1.1 as possibly having an impact on the DBR model results, only the lack of ROMPCS emplacement between Panels 3, 4, 5, 6, and 9, modeled as the southernmost panel closure area has a direct impact on the DBR calculation methodology. However, the DBR model results are also influenced by other changes to the CRA-2019 PA through their effects on the CRA-2019 Salado flow model output that are used to initialize the DBR model pressure and saturation conditions, and the borehole areas calculated by CUTTINGS_S.

This analysis shows that the average and maximum DBR volumes from the CRA-2019 PA are significantly higher than those from the CRA-2014 PA. The increases in mean DBR volume are primarily accounted for in the E1 intrusion scenarios, in which the repository is hydraulically connected to an underlying pressurized brine pocket by an intersecting borehole. In the CRA-2014 PA, as in those before it, the lower intrusions, those into the panel with the prior E1 intrusion, accounted for the majority of the total DBR release volume. This is still the case in the CRA-2019 PA, but substantial increases in the middle intrusions release volumes result in them now representing a much more significant minority of the total. Release volumes from Upper intrusions in all scenarios remain small, as do release volumes from intrusions in the undisturbed repository scenario and from intrusions in both E2 intrusion scenarios.

These changes appear to be driven by differences in the initial conditions derived from the BRAGFLO Salado model, particularly those that create increased brine pressure in the lower intrusion region, and increased brine pressure and saturation in the middle intrusion region. These results show that intrusions into the middle region now meet the minimum pressure and saturation thresholds for a DBR event, when they did not before. Additionally, once the pressure and saturation thresholds are met, higher saturation can move the flow regime from a gas dominated to a brine dominated or all brine flow regime, in which higher pressures correlate with higher release volumes.

Furthermore, because the correlations of DBR volume to intruded panel conditions remain similar between CRA-2019 and CRA-2014, the emplacement of PCS_NO material in panel closures in the south does not appear to be changing any fundamental relationship between adjacent panel conditions and DBR release volumes. In other words, adjacent panels do not appear to be lending significantly more pressure support over the abandoned panel closures than they did over ROMPCS panel closures. The faster pressure equilibration time across PCS_NO in the BRAGFLO Salado model appears to be a more important controlling variable for DBR volumes.

This page intentionally left blank

7.0 REFERENCES

- Brooks, R.H. and A.T. Corey. 1964. Hydraulic properties of porous media, Hydrology Paper no. 3, Civil Engineering Department, Colorado State University, Fort Collins, CO.
- Clayton, D.J., S. Dunagan, J.W. Garner, A.E. Ismail, T.B. Kirchner, G.R. Kirkes, M.B. Nemer. 2008. Summary Report of the 2009 Compliance Recertification Application Performance Assessment. Sandia National Laboratories, Carlsbad, NM. ERMS 548862.
- Clayton, D.J., R.C. Camphouse, J.W. Garner, A.E. Ismail, T.B. Kirchner, K.L. Kuhlman, M.B. Nemer. 2010. Summary Report of the CRA-2009 Performance Assessment Baseline Calculation. Sandia National Laboratories, Carlsbad, NM. ERMS 553039.
- Cotsworth, E. 2005. EPA Letter on Conducting the Performance Assessment Baseline Change (PABC) Verification Test. U.S. EPA, Office of Radiation and Indoor Air, Washington, D.C. ERMS 538858.
- Cotsworth, E. 2009. EPA Letter on CRA-2009 First Set of Completeness Comments. U.S. EPA, Office of Radiation and Indoor Air, Washington, D.C. ERMS 551444.
- Day, B. 2019. Analysis Package for Salado Flow in the 2019 Compliance recertification Application Performance Assessment (CRA-2019 PA). Sandia National Laboratories, Carlsbad, NM. ERMS 571368.
- Kicker, D. 2019. Analysis Package for Cuttings, Cavings, and Spallings in the 2019 Compliance Recertification Application Performance Assessment (CRA-2019 PA). Sandia National Laboratories, Carlsbad, NM. ERMS 571369.
- Kim, S. and M. Feng. 2019. Input Parameter Report for the 2019 Compliance Recertification Application Performance Assessment (CRA-2019 PA). Sandia National Laboratories, Carlsbad, NM. ERMS 571377.
- Kirchner, T. 2013. Generation of the LHS Samples for the CRA-2014 (AP-164) PA Calculations. Sandia National Laboratories, Carlsbad, NM. ERMS 559950.
- Kirchner, T., A. Gilkey, and J. Long. 2014. Summary Report on the Migration of the WIPP PA Codes from VMS to Solaris, AP-162 Revision 1. Sandia National Laboratories, Carlsbad, NM. ERMS 561757.
- Kirchner, T., A. Gilkey, and J. Long. 2015. Addendum to the Summary Report on the Migration of the WIPP PA Codes from VMS to Solaris, AP-162. Sandia National Laboratories, Carlsbad, NM. ERMS 564675.
- Lee, J. 1982. Well Testing. SPE Textbook Series Vol. 1. New York, NY: Society of Petroleum Engineers of AIME.
- Leigh, C.D., J.F. Kanney, L.H. Brush, J.W. Garner, G.R. Kirkes, T. Lowry, M.B. Nemer, J.S. Stein, E.D. Vugrin, S. Wagner, and T.B. Kirchner. 2005. 2004 Compliance Recertification Application Performance Assessment Baseline Calculation, Revision 0. Sandia National Laboratories, Carlsbad, NM. ERMS 541521.

**ANALYSIS PACKAGE FOR DIRECT BRINE RELEASE IN THE 2019 COMPLIANCE
RECERTIFICATION APPLICATION PERFORMANCE ASSESSMENT (CRA-2019 PA)
Rev. 0, ERMS 571370**

- Long, J. 2019. Computational Code Execution and File Management for the 2019 Compliance Recertification Application Performance Assessment (CRA-2019 PA). Sandia National Laboratories, Carlsbad, NM. ERMS 571375.
- MacKinnon, R.J., and G. Freeze. 1997a. Summary of EPA-Mandated Performance Assessment Verification Test (Replicate 1) and Comparison With the Compliance Certification Application Calculations, Revision 1. Sandia National Laboratories, Carlsbad, NM. ERMS 422595.
- MacKinnon, R.J., and G. Freeze. 1997b. Summary of Uncertainty and Sensitivity Analysis Results for the EPA-Mandated Performance Assessment Verification Test, Rev. 1. Sandia National Laboratories, Carlsbad, NM. ERMS 420669.
- MacKinnon, R.J., and G. Freeze. 1997c. Supplemental Summary of EPA-Mandated Performance Assessment Verification Test (All Replicates) and Comparison With the Compliance Certification Application Calculations, Revision 1. Sandia National Laboratories, Carlsbad, NM. ERMS 414880.
- Malama, B. 2013. Analysis Package for Direct Brine Releases: CRA-2014 Performance Assessment (CRA-2014 PA). Sandia National Laboratories, Carlsbad, NM, ERMS 560069.
- Mattax, C.C. and R.L. Dalton. 1990. Reservoir Simulation. Henery L. Doherty Memorial Fund Society of Petroleum Engineers Inc., Richardson, TX.
- Pasch, J. and C. Camphouse, 2011. Analysis Package for Direct Brine Releases: Panel Closure Redesign and Repository Reconfiguration Performance Assessment (PC3R PA), Revision 0. Sandia National Laboratories. Carlsbad, NM. ERMS 555249.
- Stoelzel, D.M. and D.G. O'Brien. 1996. Conceptual Model Description of BRAGFLO Direct Brine Release Calculations to Support the Compliance Certification Application (CCA MASS Attachment 16-2). U.S. Department of Energy, Carlsbad, NM. ERMS 239090.
- U.S. Congress. 1992. WIPP Land Withdrawal Act, Public Law 102-579, 106 Stat. 4777, 1992; as amended by Public Law 104-201, 110 Stat. 2422, 1996.
- U.S. Department of Energy (DOE) 1996. Title 40 CFR Part 191 Compliance Certification Application for the Waste Isolation Pilot. U.S. Department of Energy Waste Isolation Pilot Plant, Carlsbad Area Office, Carlsbad, NM. DOE/CAO-1996-2184.
- U.S. Department of Energy (DOE) 2004. Title 40 CFR Part 191 Compliance Recertification Application for the Waste Isolation Pilot Plant, , 10 vols., U.S. Department of Energy Waste Isolation Pilot Plant, Carlsbad Area Office, Carlsbad, NM. DOE/WIPP 2004-3231.
- U.S. Environmental Protection Agency (EPA). 1998. 40 CFR 194, Criteria for the Certification and Recertification of the Waste Isolation Pilot Plant's Compliance with the Disposal Regulations: Certification Decision: Final Rule, Federal Register. Vol. 63, 27354-27406.
- U.S. Environmental Protection Agency (EPA). 2006. 40 CFR 194, Criteria for the Certification and Recertification of the Waste Isolation Pilot Plant's Compliance with the Disposal Regulations: Certification Decision: Final Rule, Federal Register. Vol. 71, 18010-18021.
- U.S. Environmental Protection Agency (EPA). 2010. 40 CFR Part 194 Criteria for the Certification and Recertification of the Waste Isolation Pilot Plant's Compliance With the

ANALYSIS PACKAGE FOR DIRECT BRINE RELEASE IN THE 2019 COMPLIANCE
RECERTIFICATION APPLICATION PERFORMANCE ASSESSMENT (CRA-2019 PA)
Rev. 0, ERMS 571370

Disposal Regulations: Recertification Decision, Federal Register No. 222, Vol. 75, pp. 70584-70595, November 18, 2010.

U.S. Environmental Protection Agency (EPA). 2017. Criteria for the Certification and Recertification of the Waste Isolation Pilot Plant's Compliance with the Disposal Regulations; Recertification Decision. July 19, 2017. Office of Radiation and Indoor Air, Docket EPA-HQ-OAR-2014-0609-0079.

Zeitler, T.R., B. Day, J. Bethune, R. Sarathi, J. Long. 2017. Assessment of Abandoned Panel Closures in South End of Repository and Lack of Waste Emplacement in Panel 9. Sandia National Laboratories. Carlsbad, NM. ERMS 568459.

Zeitler, T.R. 2019. Analysis Plan for the 2019 WIPP Compliance Recertification Application Performance Assessment. Sandia National Laboratories, Carlsbad, NM. ERMS 571150.

This page intentionally left blank.